Effects of Grain Boundary Disorder on Dislocation Emission

Valery Borovikov[1], Mikhail I. Mendelev[1] and Alexander H. King[1,2]
[1]*Division of Materials Sciences and Engineering, Ames Laboratory, Ames, IA 50011*
[2]*Department of Materials Science and Engineering, Iowa State University, Ames, IA 50011*

It was recently reported that segregation of Zr to grain boundaries (GB) in nanocrystalline Cu can lead to the development of disorder in the intergranular structure [1,2]. In this study we employ atomistic computer simulations to investigate how this disorder affects dislocation nucleation from the GBs under applied stress. It was found that a fully disordered grain boundary structure suppresses dislocation emission and significantly increases the yield stress. Depending on the solute concentration and heat-treatment, however, partial disorder may also occur and this aids dislocation nucleation rather than suppressing it, reducing or eliminating the strengthening effect.

The addition of low-solubility elements that segregate to grain boundaries (GB) can stabilize a nanocrystalline material against grain growth, suppress grain boundary mediated plasticity and improve the fatigue characteristics of the material [3-9]. Zr has been found to strongly segregate to GBs in nanocrystalline Cu, and is effective at stabilizing it at elevated temperatures [10]. This segregation has also been shown to lead to the formation of amorphous intergranular films under certain annealing conditions [1,2]. It was also recently demonstrated that solute segregation can affect a GB's ability to emit dislocations [11]. Emission of dislocations from GBs is a key deformation mechanism for many nano/poly-crystalline materials [12,13], so segregating solutes that stabilize the microstructure against coarsening can also increase the yield strength. In this letter, we describe a set of molecular dynamics (MD) simulations, which demonstrate that the effect of Zr on dislocation nucleation in nano-Cu depends on the nature of the disorder at GBs, which is determined by the thermal history of the sample.

The MD simulations were performed using the semi-empirical potential developed in [14]. A bi-crystal geometry, with two $\Sigma11(332)[110]$ symmetric tilt grain boundaries (STGB) was utilized (see Fig. 1a). This STGB contains E structural units [15], which are known to serve as the dislocation nucleation sources under applied stress [16,17]. All simulations were performed using LAMMPS [18] and the visualization was performed using OVITO [19]. The simulation cell size ($19.3\times18.5\times33.8$ nm^3) was sufficiently large to minimize the effect of periodic boundary conditions on the dislocation nucleation [16,20]. The distribution of Zr atoms at the GBs was equilibrated at 300 K using the hybrid Monte Carlo/ molecular dynamics technique [21]. Further details of the preparation of the initial models can be found in [11] and the discussion of the Zr segregation pattern can be found in [14]. Additional models were prepared by annealing the initial models at 900 K for 10 ns, followed by rapid quenching to 300 K and equilibrating at this temperature.

Tensile loading simulations were carried out at 300 K, with a constant engineering strain rate of 10^8 s^{-1} applied to the z direction. The stresses in the other two directions were held at zero. As strain is applied, the stress initially increases, then reaches a peak and drops when the first dislocation is emitted from the GB. The peak stress value was regarded as the yield stress in the present study. Figure 1b shows the effects of solute concentration on the yield stress. For the unannealed specimens, the yield stress reaches a peak near at ~0.83% Zr and then decreases with further solute additions such that the models with the largest Zr content have almost the same yield stress as pure Cu. For the annealed specimens, Zr additions cause increases in the yield stress exceeding those of the unannealed specimens for all concentrations greater than ~0.3%. The strengthening effect is monotonic up to a concentration of ~1 %, beyond which the effect of increasing Zr concentration is not significant, although there is no systematic loss of yield strength as seen in the unannealed cases.

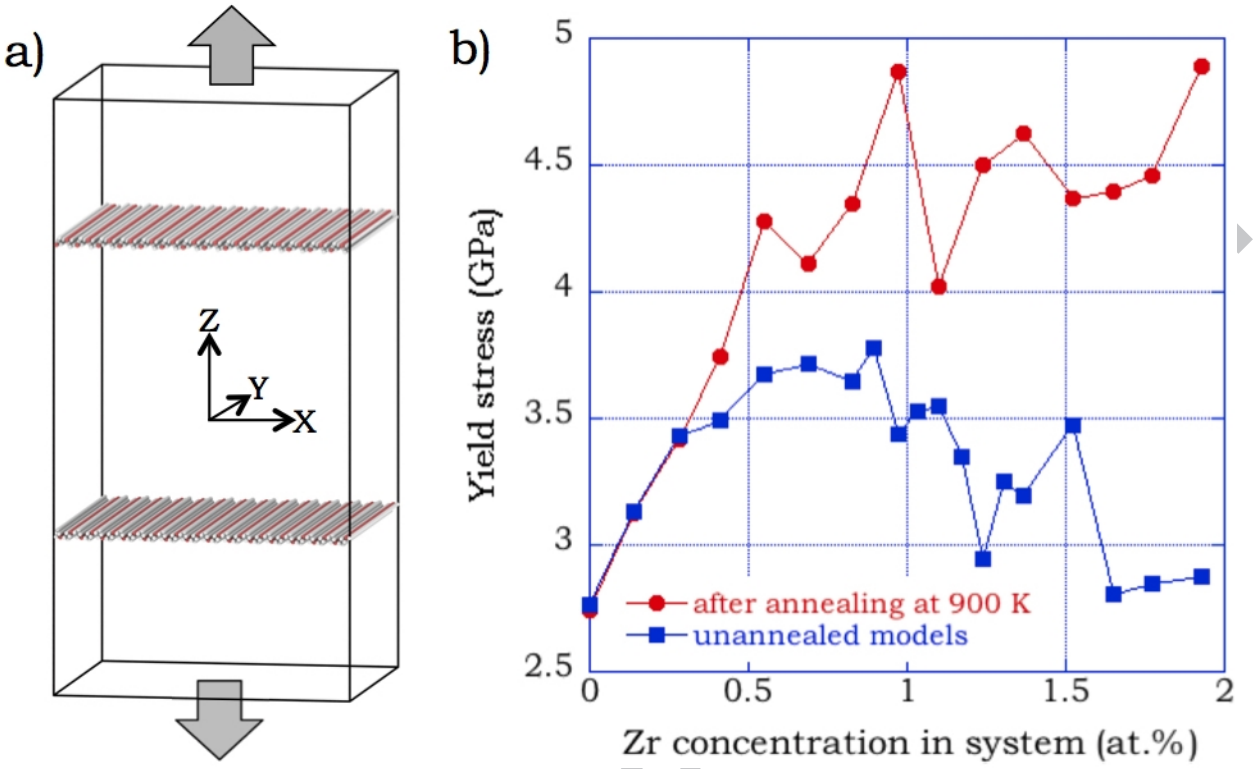

Figure 1. a) Cartoon of the simulation cell. b) The yield stress as function of the solute concentration for unannealed and annealed models.

To explain the obtained result we now turn to the changes in the GB structure associated with the Zr segregation. Annealing does not change the GB structure in pure Cu (see Fig. 2) but can alter it in the presence of Zr, so the difference between the yield stresses obtained for the initial and annealed models can be attributed to the presence of the Zr solutes. The addition of a small amount of Zr (up to 0.28 %) does not significantly change the GB structure even after the annealing, and the MD simulations show almost the same yield stresses for unannealed and annealed specimens in this concentration range.

For the unannealed model, the presence of solutes modifies the GB structure when the Zr concentration is greater than 0.83 % (see Fig. 2). The boundary still retains E units where the dislocations can nucleate, but these are surrounded by disordered regions (which resembles the description originally proposed by Mott to explain the kinetics of grain boundary sliding and migration [22]). This structure makes dislocation nucleation easier because the atoms in the amorphous regions around the E unit can readily rearrange to accommodate the atomic shifts associated with the emission of a dislocation. To illuminate the effect, we compare the atomic displacements, which occur upon dislocation emission in the cases of lower (0.28%) and higher (1.36%) Zr concentrations. In both cases, we measure displacements by the changes in the atomic coordinates during the time interval of 22 ps, which covers the emission event. Figure 3 shows that for the lower Zr concentration, dislocation emission does not lead to significant atomic reshuffling in the GB region because the ordered, periodic GB structure does not allow such rearrangement.

For higher Zr concentration: the GB structure is partially disordered; dislocation nucleation is easily accommodated by atomic reshuffling and requires a smaller applied stress. This explains the decrease of the yield stress at larger Zr concentrations. Figure 2 shows that further increases of the Zr concentration lead to increasing amorphization of the GB structure, but some E units persist as ordered regions, and dislocation nucleation becomes easier, with the increasing amorphous volume, leading to the decrease in the yield stress (see Fig. 1b).

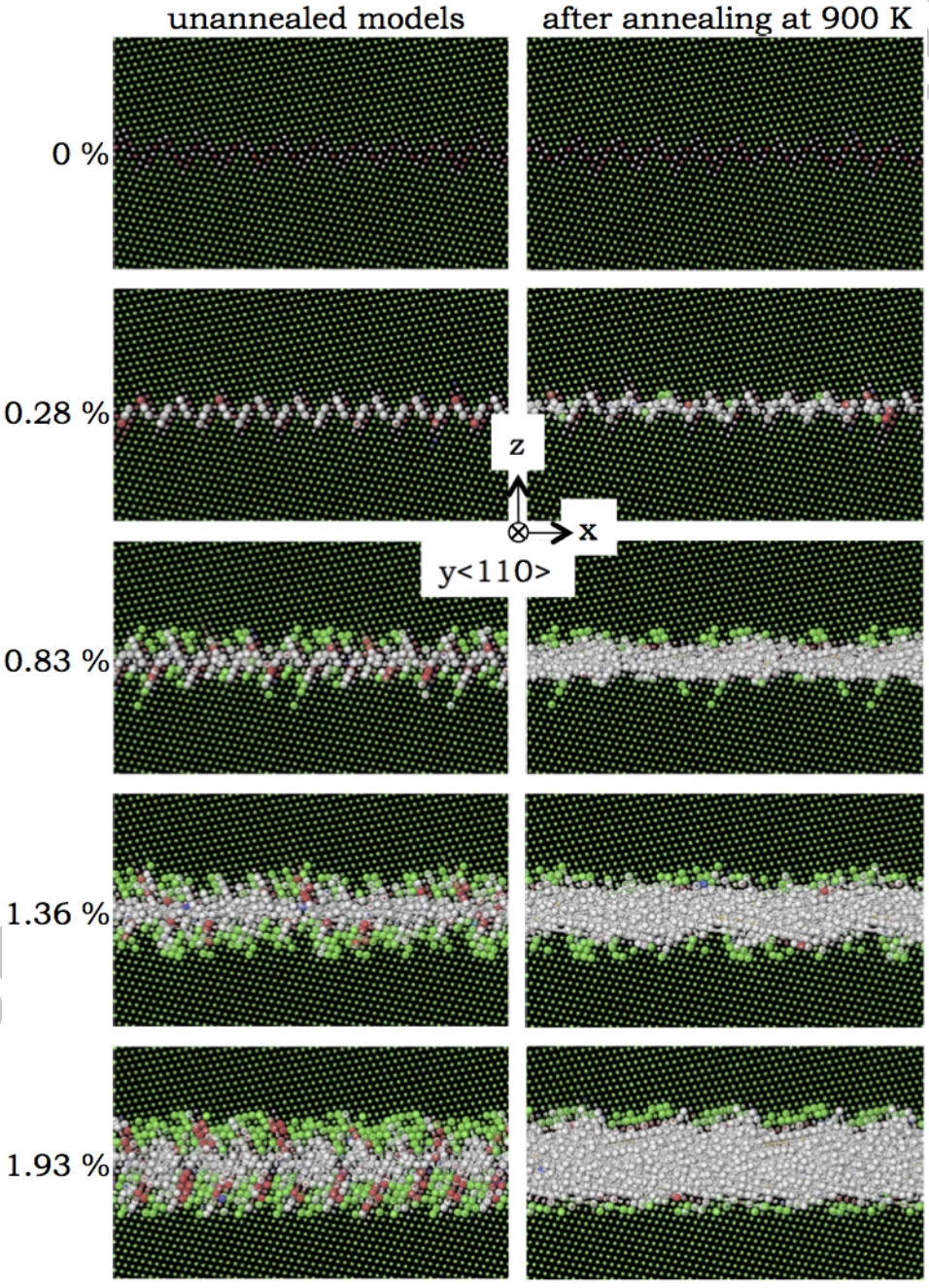

Figure 2. The GB structure just before the emission of the first dislocation. The size of the Cu atoms is artificially decreased to show the positions of the Zr atoms. The atoms are colored according to the common neighbor analysis (CNA) [23,24]. The color-coding is the following: green – fcc, red – hcp, grey – other. Stacking fault segments (shown in red) at the GB indicate the preexisting dislocation embryos.

Annealing the initial model at T=900 K makes the GB structure fully amorphous when the Zr concentration is above 0.83 % (see Fig. 2). Now the GB does not contain the dislocation embryos originally present at the GB in the form of the E structural units [25,26]. In the absence of these dislocation embryos it becomes difficult to nucleate a dislocation from the GB, which leads to a very high yield stress. Further addition of Zr makes the GB region wider but does not create new dislocation sources, and the yield stress does not change systematically at larger Zr concentrations.

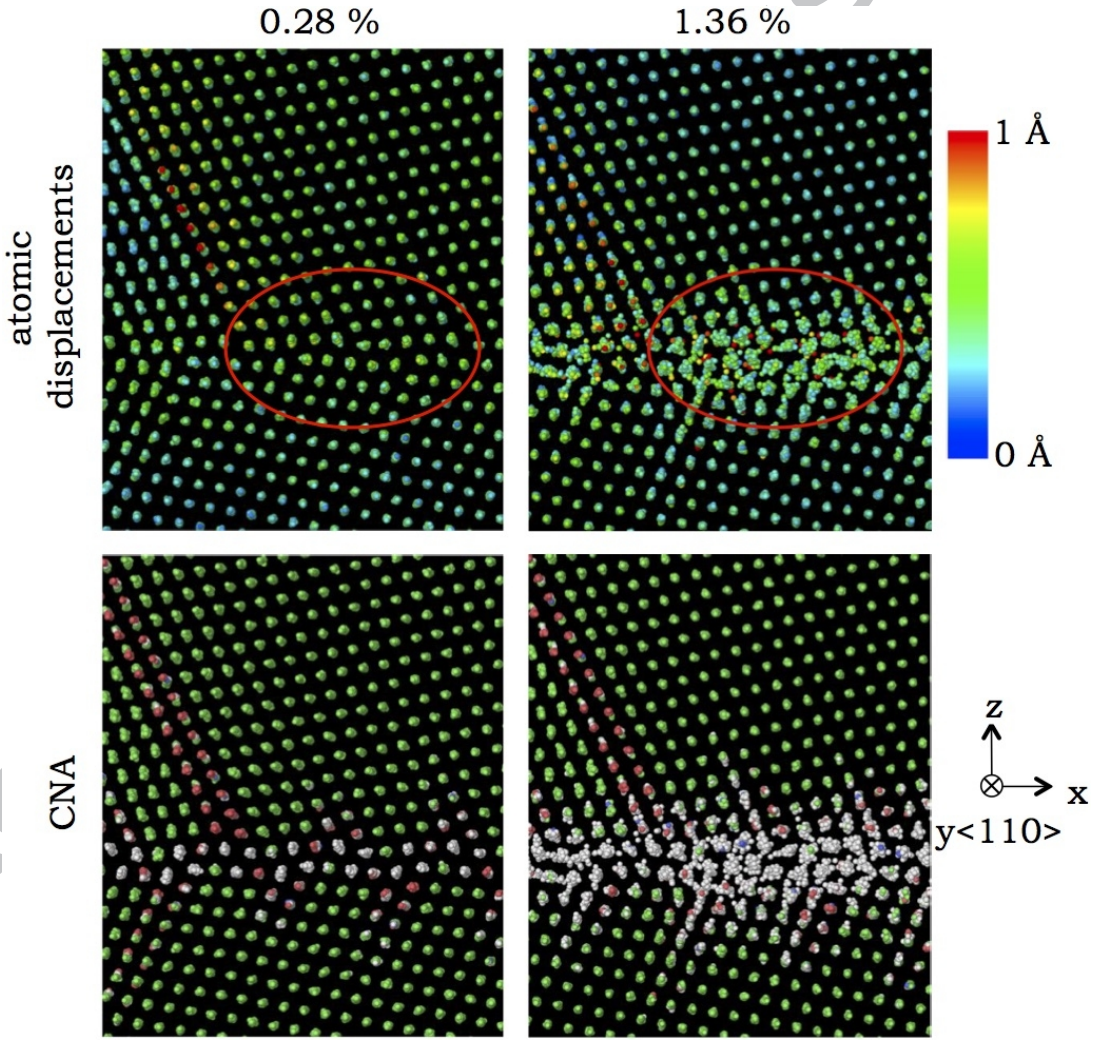

Figure 3. The region of the GB where the first dislocation was emitted for the cases of lower (0.28%) and higher (1.36%) Zr concentrations (unannealed models). The upper images show the atomic displacements caused by the dislocation emission from the GB under applied tensile

loading (at T=300K). The size of both solutes and solvents is decreased (and made the same). The coloring scheme in the lower images is the same as in Fig. 2.

In summary, our simulations elucidate the effects of solute-induced disordering of the GB structure on dislocation nucleation. If disorder is complete and the GB does not retain any dislocation embryos, the yield stress is increased because of the lack of dislocation nucleation sites. Partial disorder can lead to dramatic decreases in the yield stress if some dislocation embryos remain within the GB, because the atomic shuffling in amorphous regions near the dislocation sources aids the dislocation emission.

Complete disorder was achieved in the case of a Zr-segregated at Σ11(332)[110] GB in Cu, by annealing at T=900 K for 10 ns. Experimental observations may vary because much longer annealing can lead to the formation of Cu-Zr compounds and the interfaces between these compounds and the bulk Cu can provide new dislocation nucleation sites, as discussed in [27]. The average Zr concentration corresponding to a particular grain boundary composition is also likely to depend on the grain size. Identifying optimal compositions and annealing conditions for coarsening resistance and/or strengthening will require further investigation, guided by understanding the effects described here.

Acknowledgements:

This work was supported by the U.S. Department of Energy, Office of Science, Basic Energy Sciences, Materials Science and Engineering Division. The research was performed at Ames Laboratory, which is operated for the U.S. DOE by Iowa State University under contract # DE-AC02-07CH11358

References:

[1] A. Khalajhedayati, Z. L. Pan, and T. J. Rupert, Nature Communications 7 (2016) 8 10802.
[2] A. Khalajhedayati and T. J. Rupert, Jom 67 (2015) 2788.
[3] T. Chookajorn, H. A. Murdoch, and C. A. Schuh, Science 337 (2012) 951.
[4] T. Frolov, K. A. Darling, L. J. Kecskes, and Y. Mishin, Acta Materialia 60 (2012) 2158.
[5] K. A. Darling, M. A. Tschopp, B. K. VanLeeuwen, M. A. Atwater, and Z. K. Liu, Computational Materials Science 84 (2014) 255.
[6] P. C. Millett, R. P. Selvam, and A. Saxena, Materials Science and Engineering a-Structural Materials Properties Microstructure and Processing 431 (2006) 92.
[7] R. I. Babicheva, S. V. Dmitriev, D. V. Bachurin, N. Srikanth, Y. Zhang, S. W. Kok, and K. Zhou, International Journal of Fatigue 102 (2017) 270.
[8] R. I. Babicheva, S. V. Dmitriev, L. C. Bai, Y. Zhang, S. W. Kok, G. Z. Kang, and K. Zhou, Computational Materials Science 117 (2016) 445.

[9] A. V. Zinovev, M. G. Bapanina, R. I. Babicheva, N. A. Enikeev, S. V. Dmitriev, and K. Zhou, Physics of Metals and Metallography 118 (2017) 65.
[10] M. A. Atwater, R. O. Scattergood, and C. C. Koch, Materials Science and Engineering a-Structural Materials Properties Microstructure and Processing 559 (2013) 250.
[11] V. Borovikov, M. I. Mendelev, and A. H. King, International Journal of Plasticity 90 (2017) 146.
[12] B. Chen, K. Lutker, S. V. Raju, J. Y. Yan, W. Kanitpanyacharoen, J. L. Lei, S. Z. Yang, H. R. Wenk, H. K. Mao, and Q. Williams, Science 338 (2012) 1448.
[13] J. Chen, L. Lu, and K. Lu, Scripta Materialia 54 (2006) 1913.
[14] V. Borovikov, M. I. Mendelev, and A. H. King, arXiv:1712.07596 (2018).
[15] J. D. Rittner and D. N. Seidman, Physical Review B 54 (1996) 6999.
[16] D. E. Spearot, M. A. Tschopp, K. I. Jacob, and D. L. McDowell, Acta Materialia 55 (2007) 705.
[17] M. A. Tschopp, G. J. Tucker, and D. L. McDowell, Acta Materialia 55 (2007) 3959.
[18] S. Plimpton, Journal of Computational Physics 117 (1995) 1.
[19] A. Stukowski, Modelling and Simulation in Materials Science and Engineering 18 (2010) 015012.
[20] D. E. Spearot, K. I. Jacob, and D. L. McDowell, International Journal of Plasticity 23 (2007) 143.
[21] B. Sadigh, P. Erhart, A. Stukowski, A. Caro, E. Martinez, and L. Zepeda-Ruiz, Physical Review B 85 (2012) 184203.
[22] N. F. Mott, Proceedings of the Physical Society of London 60 (1948) 391.
[23] J. D. Honeycutt and H. C. Andersen, Journal of Physical Chemistry 91 (1987) 4950.
[24] A. Stukowski, Modelling and Simulation in Materials Science and Engineering 20 (2012) 045021.
[25] V. Borovikov, M. I. Mendelev, A. H. King, and R. LeSar, Journal of Applied Physics 117 (2015) 085302.
[26] L. Smith and D. Farkas, Philosophical Magazine 94 (2014) 152.
[27] V. Borovikov, M. I. Mendelev, and A. H. King, Scripta Materialia 154 (2018) 12.